



OPEN ACCESS

EDITED BY

Zimin Li,
Chinese Academy of Sciences (CAS), China

REVIEWED BY

Hongjian Zhu,
Yanshan University, China
Mohsina Anjum,
Bihar Agricultural University, India

*CORRESPONDENCE

Jörg Schaller,
✉ joerg.schaller@zalf.de

RECEIVED 09 October 2025

REVISED 06 January 2026

ACCEPTED 13 January 2026

PUBLISHED 27 January 2026

CITATION

Stein M, Kilian Salas S, Kleeberg R, Jungkunst HF and Schaller J (2026) Opportunities and challenges of sequential extraction of silicon in contrasting soils.

Front. Environ. Sci. 14:1721752.
doi: 10.3389/fenvs.2026.1721752

COPYRIGHT

© 2026 Stein, Kilian Salas, Kleeberg, Jungkunst and Schaller. This is an open-access article distributed under the terms of the [Creative Commons Attribution License \(CC BY\)](#). The use, distribution or reproduction in other forums is permitted, provided the original author(s) and the copyright owner(s) are credited and that the original publication in this journal is cited, in accordance with accepted academic practice. No use, distribution or reproduction is permitted which does not comply with these terms.

Opportunities and challenges of sequential extraction of silicon in contrasting soils

Mathias Stein^{1,2}, Simone Kilian Salas³, Reinhard Kleeberg⁴, Hermann F. Jungkunst³ and Jörg Schaller^{1*}

¹Leibniz Center for Agricultural Landscape Research (ZALF), Müncheberg, Germany, ²Just Transition Center (JTC), Halle, Germany, ³ES Landau, RPTU Kaiserslautern-Landau, Landau, Germany, ⁴TU Bergakademie Freiberg, Institute of Mineralogy, Freiberg, Germany

Introduction: The importance of silicon for soil functioning has only recently received the attention it deserves in soil science (and ecology). To identify the actual effects of Si on ecosystem functioning, a precise knowledge about different Si soil fractions (plant-available, amorphous Si, and Si bound to organic matter, short-range ordered aluminosilicates (SROAS), or iron oxides/hydroxides) is required. Sequential extraction techniques are a common tool to quantify different soil fractions in soils of humid-temperate climates, whereas their reliability in other climatic zones or contrasting soils remains unclear. This study tested to what extent sequential extraction is applicable on soils from the High Andes and Amazon Basin, two contrasting regions with distinct soil formation processes.

Methods: To ensure method validity, we analyzed Si, iron (Fe), and aluminum (Al) in extracts and conducted X-ray diffraction (XRD) to detect mineral changes pre- and postextraction. Amorphous Si was more abundant in the High Andes soils, yet plantavailable Si was unexpectedly lower compared to Amazon Basin soils.

Results: Silicon occluded in Fe oxides/hydroxides or SROAS showed no differences between the two contrasting soils. XRD results revealed the following limitations: dithionite extraction did not completely remove Fe from hematite in Andean soils, and powder XRD lacked precision for amorphous Si quantification. Among the tested methods, CaCl₂ extraction (for plant-available Si) and a two-step protocol—density separation for biogenic Si (bASi), followed by Tiron extraction for total amorphous Si (tASi)—were the most effective for these soils.

Discussion: These findings, with different methods not being able to characterize the soil used, underscore the need to refine Si extraction techniques for environments. Expanding methods originally developed in temperate soils is critical to understanding Si's role in biogeochemical cycles and its broader significance for different ecosystem performance.

KEYWORDS

amorphous silica, sequential extraction methods, silica cycling, soil silicon, wet chemical extraction

1 Introduction

Silicon (Si), despite its ubiquitous presence in terrestrial and marine environments, has only recently been gaining adequate recognition in soil and plant sciences. Its full significance has yet to be explored (Cooke and Leishman, 2011; Schaller et al., 2021; de Tombeur et al., 2023; Schaller et al., 2024; Schaller et al., 2025). Silicon is the second most abundant element in Earth's crust (Wedepohl, 1995) and is found in myriads of forms in various soil fractions

shaped by soil formation processes, making it a key element in biogeochemical cycling. Si availability in soil depends for example on soil age, microbial turnover and aggregation (Derry et al., 2005; Li et al., 2022; Puppe et al., 2022). Studies revealed that Si enhances plant phosphorus availability (Schaller et al., 2022) and amorphous Si increases water retention and plant-available water in sandy soils (Schaller et al., 2020). Consequently, quantifying these Si fractions is essential to unravel processes involving Si and their specific biogeochemical roles for different ecosystems and climate zones.

Complementary to the growing interest in Si, methods to analyze the different Si fractions in soils are also continuously evolving, yet, without unified consensus. Most Si in terrestrial environments resides in primary silicates (e.g., feldspars, micas, quartz) or secondary clay minerals. Weathering of minerals releases dissolved silicic acid (monomeric and polymeric forms), which is also released by the decomposition of biogenic amorphous silica (bASi) derived from plants, minerogenic amorphous silica (mASi) precipitated on mineral surfaces, and short-range ordered aluminosilicates (SROAS) (Schaller et al., 2021). Silicic acid exists in a dynamic equilibrium influenced by Si concentration, pH, temperature, and ionic strength (Dietzel, 2002). Adsorption onto soil components, particularly iron oxides/hydroxides, may be more pronounced for polymeric silicic acid (Schaller et al., 2021).

To characterize these fractions, either single and/or sequential extraction methods have been applied (Schaller et al., 2021; Stein et al., 2024). Sequential extraction procedures allow the operational separation of element pools in soils, enabling insights into their potential mobility, bioavailability, and binding forms. However, these methods are prone to cumulative errors, incomplete selectivity of reagents, and potential redistribution or loss of analytes during washing steps, which can compromise the interpretation of individual fractions. Georgiadis et al. (2013), Georgiadis et al. (2015) introduced a sequential extraction method, validated on pure minerals and temperate-humid soils. In this study, the protocol was slightly modified to account for specific mineralogical characteristics of tropical soils. In particular, dithionite-citrate-bicarbonate (DCB) extraction (Mehra and Jackson, 1958) was included to dissolve crystalline iron oxides such as hematite, which are common in tropical soils but rare in soils of temperate climates and are not fully dissolved by ammonium oxalate (Rennert, 2019). Acetic acid extraction was excluded due to overlap with CaCl_2 extractions for adsorbed Si (Georgiadis et al., 2014), and 0.2 M sodium hydroxide was replaced with 0.1 M Tiron for biogenic and minerogenic ASi as it showed comparable effectiveness and selectivity targeting ASi (Stein et al., 2024).

The objective of this study was to evaluate whether a slightly adapted sequential extraction method, based on the protocol of Georgiadis et al. (2013) developed for humid-temperate soils, is suitable for quantifying silicon pools in soils with contrasting pedogenic and mineralogical characteristics, particularly those typical of tropical regions. If this method would be reliable for all soil, using this method would be a solid basis for improving models on the global silicon cycle. We tested this sequential extraction method on two contrasting soils: High Andes soils (HA-soils) and Amazon Basin soils (AB-soils). HA-soils, classified as Phaeozems and Umbrisols, are shallow and weakly developed, forming from andesitic parent material rich in plagioclase, pyroxene, and hornblende (Mamani et al., 2010; Szymański and Szkaradek,

2018). In contrast, AB-soils, classified as Ferralsols and Acrisols dominated by Fe and Al oxides (e.g., goethite, hematite) and kaolinite clays, with low organic carbon and nutrient contents (Souza et al., 2017). To ensure the validity of the extraction method and to explicitly assess extractant selectivity, we quantified silicon (Si), iron (Fe), and aluminum (Al) in all extracts. In addition, powder X-ray diffraction (XRD) analyses were conducted to identify changes in mineral composition before and after the sequential extraction procedure, an approach that have rarely been included in studies of sequential Si extraction.

We hypothesize that the adapted sequential extraction protocol maintains sufficient selectivity and effectiveness to differentiate Si fractions in soils formed under diverse pedoclimatic conditions.

2 Materials and methods

2.1 Area description and soil sampling

Soil samples from the High Andes (HA) were collected in the Cordillera Urubamba near the locality of “CanchaCancha” in Peru ($13^{\circ}14'35''\text{S}$, $72^{\circ}1'18''\text{W}$) at approximately 4,500 m above sea level. The region experiences low mean annual temperatures ($5^{\circ}\text{C} \pm 5^{\circ}\text{C}$), characterized by high diurnal variations with midday peaks of 5°C – 15°C . A pronounced dry season occurs from May to October (Troll, 1968; Heitkamp et al., 2014). Soil samples were collected to a depth of 40 cm across various vegetation types (rangeland, grassland, forest) within 500 m of each other to minimize spatial variability. Each land-use was sampled in three site replicates, with one to two depth increments sampled down to 40 cm, resulting in a total of 13 samples for HA-soil. The soil types in the rangeland and grassland were classified as Umbrisols and in the forest sites as Phaeozems (Heitkamp et al., 2014).

In the Amazon Basin (AB), soil samples were collected near the locality of “Empresaña” in Bolivia ($11^{\circ}28'11''\text{S}$, $68^{\circ}49'17''\text{W}$) at approximately 300 m above sea level. This region is characterized by a tropical climate with a mean annual temperature of $\sim 25^{\circ}\text{C}$ and mean annual rainfall exceeding 1,500 mm (Wright and Bennema, 1965). Precipitation decreases regionally from west to east (Espinoza Villar et al., 2009), and during the dry season (May to September), rainfall often falls below 100 mm per month (Toledo et al., 2011). For each vegetation type (primary forest, secondary forest, bushy pasture, pasture), one soil pit was established, with a minimum distance of 200 m between adjacent pits. Bulk soil samples were collected to a depth of 1 m in each pit. Each land-use type was represented by one site replicate, where bulk soil was collected from three depths down to 70 cm within a soil pit, resulting in a total of 12 samples within AB-soil. Acrisols and Ferralsols are the two dominant soil types in the area (Cochrane et al., 2010) and both were sampled and were equally distributed across land-uses. In total, 25 soil samples were taken, and all extraction steps were performed individually on each sample.

2.2 Sequential extraction

To quantify different silicon (Si) fractions in the soil, a modified protocol based on Georgiadis et al. (2013) was followed. We

modified the protocol to improve accuracy in quantifying Si bound to crystalline iron oxides by incorporating dithionite–citrate–bicarbonate (DCB) extraction (Mehra and Jackson, 1958), which more effectively dissolves crystalline phases like hematite, compared with ammonium oxalate. Acetic acid extraction was excluded to avoid overlap with CaCl₂-extractable Si as recommended by (Georgiadis et al., 2014). Additionally, 0.1 M Tiron replaced 0.2 M sodium hydroxide for biogenic and minerogenic ASi as it is as effective and selective targeting ASi (Stein et al., 2024).

Prior to extraction, samples were air-dried and sieved to 2 mm. Following each extraction step, samples were centrifuged at 4,500 g and filtered through 0.45 μm membrane filters. Except for the first step, samples were thoroughly washed twice with Milli-Q water to remove residual extractants. Readily available Si was determined using 0.01 M CaCl₂ with a 1:5 soil-to-solution ratio (1 g soil: 5 mL solution). Samples were shaken horizontally for 1 min per hour over 16 h. Silicon bound to or occluded in soil organic matter (SOM) was analysed by oxidizing SOM with H₂O₂. First, 20 mL of 17.5% H₂O₂ was added to the soil and manually shaken at ambient temperature for 1 h. Subsequently, 10 mL of 35% H₂O₂ was added, and the samples were heated in a water bath at 85 °C until the reaction was complete (cessation of gas evolution). Silicon associated with pedogenic Fe oxides and hydroxides was extracted by reductive dissolution using Dithionite-Citrate-Bicarbonate (DCB) (Mehra and Jackson, 1958). Samples were treated with 40 mL of 0.3 M sodium citrate, 5 mL of 1 M sodium bicarbonate, and 1 g sodium dithionite for 15 min at 80 °C. Short-range-ordered Al-silicates were targeted with a solution of 0.2 M ammonium oxalate and 0.2 M oxalic acid. The samples were shaken for 1 min per hour, first exposed to daylight for 8 h, and then irradiated with UV light for an additional 12 h. Biogenic amorphous silica (bASi) was separated by density fractionation using sodium polytungstate ($\rho = 2.3 \text{ g cm}^{-3}$) and subsequently extracted with 0.1 M Tiron at 80 °C for 24 h (Schaller et al., 2021). Total amorphous silica (tASi) was extracted without density fractionation using 0.1 M Tiron, and the minerogenic amorphous silica fraction (mASi) was calculated by subtracting bASi from tASi.

All samples were analyzed for Si, aluminum (Al), and iron (Fe) to evaluate potential Si-binding associations and confirm extractant selectivity. Elemental concentrations were determined using inductively coupled plasma optical emission spectrometry (Thermo Scientific iCAP 6000, U.K.).

2.3 X-ray powder diffraction (XRPD)

Given the minimal alteration of mineral composition by the weak CaCl₂ extraction, we excluded XRPD analysis for untreated samples. Due to the limited quantity of post-extraction soil samples (<1 g in most cases), detailed clay mineral analysis through size fractionation and separate XRPD measurements was not feasible. Therefore, we analyzed only bulk materials for their mineral composition.

For initial phase identification, air-dried samples were gently hand-ground in an agate mortar. Preliminary analyses focused on identifying air- and moisture-sensitive phases and assessing the general crystalline composition. For quantitative estimation of

amorphous content, two selected samples (one each from the High Andes and the Amazon Basin) were prepared with 20 mass % corundum (Pigment CR1, Baikowski) as an internal standard. These were ground with ethanol in a Retsch XRD-mill McCrone to minimize preferred orientation and maximize homogenization (Locock et al., 2012). After air-drying the slurry at ≤60 °C, the dried material was further milled in a Fritsch Pulverisette 23 to avoid aggregate formation and then passed through a 200 μm sieve. Side-loaded powder mounts were prepared to reduce preferred orientation effects during XRPD analysis (Kleeberg et al., 2008).

Diffraction patterns were recorded using an Orion P2 diffractometer (XRD Eigenmann GmbH, Schnaittach, Germany) in Bragg-Brentano mode with Co-K α radiation (40 kV, 30 mA). Measurements spanned 5°–80° 2 θ in 0.02° increments with a 2-s step time. Phase identification was conducted using the GE-Seifert ANALYZE software and the ICDD PDF-4+ database (2021). Rietveld refinement for phase quantification utilized the BGMN/PROFEX software (Bergmann et al., 1998; Döbelin and Kleeberg, 2015) with structural models adapted for stacking faults and turbostratic disorder in dioctahedral smectites and kaolinite (Ufer et al., 2004; Ufer et al. 2008; Ufer et al. 2015). Significant amorphous phases (e.g., ferrihydrite, organics, amorphous silica) were estimated indirectly as residual fractions.

2.4 Total C and TOC measurements, pH

For both sites, low pH values (measured in CaCl₂) indicated that soil carbon (C) did not contain carbonates (Vuong et al., 2013), therefore total C was measured by dry combustion at 950 °C (Truspec CHN LECO, St Joseph, MI, USA for the HA-samples and LECO RC612, RPTU Landau, Germany for the AB-samples) and total C equals total organic C (TOC).

3 Results

3.1 Soil properties

The HA-soils have a higher total organic carbon (TOC) content compared to the AB-soils, with values around 12.01% (± 3.92) and 0.66% (± 0.21), respectively. Both sites exhibited low pH values, indicating the absence of carbonates, so TOC is considered equivalent to total carbon (C). The pH values were consistently acidic across both sites, with the HA-soils having a pH of 4.3 (± 0.4), while the pH of the AB-soils was 4.1 (± 0.3).

3.2 Soil mineral composition by XRPD

The soil mineral composition, as determined by XRPD, showed distinct differences between the HA- and AB-soils (Table 1). The HA-soil exhibited a high proportion of X-ray amorphous components (45%), including organics, amorphous silica, and short-range-ordered iron hydroxides such as ferrihydrite. This was followed by plagioclase/albite, quartz, and smaller amounts of smectite, talc, vermiculite, chlorite, hematite (1.7%), and rutile. In

TABLE 1 Mineral composition of the soils from the High andes and the Amazon Basin after different steps of the sequential extractions derived by X-ray powder diffraction (XRPD) measurements.

High Andes	After CaCl ₂		After H ₂ O ₂		After Na-dithionite		After oxalate		After tiron	
Phase	%	3 σ	%	3 σ	%	3 σ	%	3 σ	%	3 σ
Plagioclase/Albite	28.5	1.2	40.0	1.8	41.6	1.5	43.3	1.5	42.6	1.5
Quartz	11.4	0.3	14.7	0.6	16.2	0.6	15.9	0.6	15.6	0.6
Hematite	1.6	0.2	1.9	0.2	1.9	0.2	1.7	0.2	1.6	0.2
Talc	3.5	0.6	4.4	0.6	4.6	0.6	4.8	0.6	5.6	0.6
Rutile	0.9	0.1	1.2	0.2	1.4	0.2	1.3	0.2	1.3	0.1
Chlorite	1.7	0.6	1.9	0.6	2.8	0.9	3.2	0.9	2.8	0.6
Vermiculite	2.1	0.9	3.3	0.9	3.2	0.9	2.5	0.9	2.4	0.9
Smectite	5.2	0.9	6.1	1.2	4.4	0.9	4.6	0.9	4.3	0.9
Amorphous	45.0	2.1	26.6	3.0	24.0	2.7	22.6	2.7	23.7	2.7
Sum	100.0		100.0		100.0		100.0		100.0	

Amazon Basin	After CaCl ₂		After H ₂ O ₂		After Na-dithionite		After oxalate		After tiron	
Phase	%	3 σ	%	3 σ	%	3 σ	%	3 σ	%	3 σ
Quartz	50.2	1.0	52.1	1.2	57.3	1.2	53.2	1.2	54.5	1.2
Gibbsite	2.1	0.4	2.1	0.5	2.9	0.6	3.0	0.6	2.8	0.6
Anatase	0.6	1.0	0.6	0.2	0.7	0.1	0.6	0.1	0.7	0.1
Kaolinite	21.8	1.7	21.1	1.7	22.7	1.3	21.7	1.3	23.0	1.1
Goethite	5.1	0.7	5.3	0.9	1.4	0.5	1.3	0.4	1.1	0.4
Hematite	0.8	0.2	0.8	0.2	0.0	0.1	0.1	0.1	0.0	0.1
Muscovite	4.5	0.6	5.0	0.6	5.3	0.6	5.4	0.6	5.5	0.6
Rutile	0.7	0.2	0.7	0.1	0.7	0.1	0.5	0.1	0.6	0.1
Amorphous	14.1	1.9	12.3	2.2	9.1	1.9	14.3	2.1	11.7	1.9
Sum	100.0		100.0		100.0		100.0		100.0	

contrast, the AB-soil had a significantly lower share of X-ray amorphous components (14.1%). The primary mineral in the AB-soil was quartz (50.2%), followed by kaolinite, goethite (5.1%), and smaller amounts of muscovite, gibbsite, hematite (0.8%), rutile, and anatase.

During the sequential extraction, the relative mineral composition of the soils changed markedly. After all extractions, the relative shares of plagioclase/albite and quartz increased to 42.6% and 15.6%, respectively, due to the dissolution of other minerals in the sample such as amorphous components, altering the proportion of specific fractions. The relative share of X-ray amorphous components decreased significantly from 45% to 23.7%, primarily due to the H₂O₂ extraction, which targets the destruction of organic matter. Surprisingly, the relative share of hematite remained unchanged throughout the sequential extraction in the HA-soil, even after DCB and oxalate extraction, which are commonly used to extract iron from pedogenic Fe oxides. All other minerals showed a relative increase during the extraction process, except smectite, which

increased during H₂O₂ extraction but subsequently decreased after DCB extraction compared to its initial share. The most pronounced decrease was observed in the X-ray amorphous components of the HA-soil.

In contrast, the AB-soil exhibited only a small decrease (2.4%) in X-ray amorphous components after all extractions. DCB extraction was more efficient in the AB-soil than in the HA-soil, as the relative hematite content dropped to 0% in the AB-soil. Goethite was not fully dissolved by DCB and oxalate but decreased by 4% during all extraction. The extractability of Fe-oxides was more efficient in the AB-soil than in the HA-soil. Surprisingly, XRPD analysis of the HA-soil did not show differences before and after Tiron extraction, despite this extraction mobilizing Si equivalent to 4.3% of the soil mass. In contrast, the AB-soil showed a decrease in X-ray amorphous components after Tiron extraction. As in the HA-soil, the AB-soil also displayed an increase in the relative share of quartz following the sequential extraction procedure. Additionally, the relative share of kaolinite and muscovite both slightly increased.

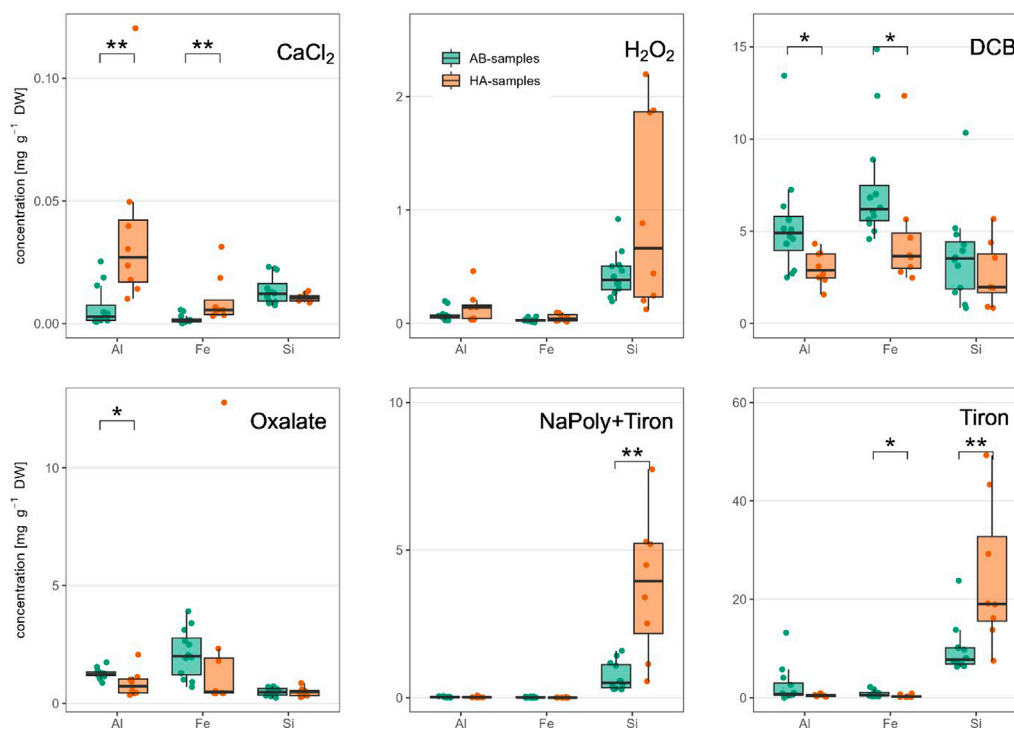


FIGURE 1
Differences in Al, Fe and Si concentrations in soil fractions between High Andes (HA) and Amazon Basin (AB). Significant differences were indicated as * ($p < 0.05$) and ** ($p < 0.01$), both by Wilcoxon test for non-parametric statistical testing.

3.3 Element content after sequential extraction

In the first sequential extraction step with CaCl₂ solution (available fraction), the element concentrations in the HA-soil were 0.01 ± 0.002 mg g⁻¹ DW for Si, 0.038 ± 0.036 mg g⁻¹ DW for Al, and 0.01 ± 0.01 mg g⁻¹ DW for Fe (Figure 1a). In contrast, the AB-soil showed significantly lower concentrations in the available fraction, with 0.007 ± 0.008 mg g⁻¹ DW for Al ($p < 0.01$, t-test) and 0.002 ± 0.002 mg g⁻¹ DW for Fe ($p < 0.05$, t-test). Si concentrations in the AB-soils, at 0.001 ± 0.005 mg g⁻¹ DW, were near detection limits and not significantly different from the HA-soils.

In the fraction bound to organic matter, Si concentrations were significantly higher in the HA-soil (0.98 ± 0.86 mg g⁻¹ DW) compared to the AB-soil (0.42 ± 0.20 mg g⁻¹ DW; $p < 0.05$, t-test; Figure 1b). No significant differences were observed for Al and Fe between the soils: HA-soil concentrations were 0.15 ± 0.14 mg g⁻¹ DW for Al and 0.05 ± 0.03 mg g⁻¹ DW for Fe, while AB-soil concentrations were 0.076 ± 0.055 mg g⁻¹ DW for Al and 0.029 ± 0.016 mg g⁻¹ DW for Fe (Figure 1b).

No significant difference in DCB-extractable Si was observed between HA-soils (2.65 ± 1.72 mg g⁻¹ DW) and AB-soils (3.68 ± 2.53 mg g⁻¹ DW; Figure 1c). However, Al content in this fraction, representing Al released by the reductive dissolution of Fe oxides, was significantly lower in HA-soils (3.01 ± 0.91 mg g⁻¹ DW) compared to AB-soils (5.38 ± 2.92 mg g⁻¹ DW; $p < 0.05$, t-test). Iron contents extracted by DCB were also lower in HA-soils (4.78 ± 3.22 mg g⁻¹ DW) than in AB-soils (7.40 ± 3.15 mg g⁻¹ DW), though the difference was not statistically significant (Figure 1c).

Silicon content in the oxalate-extractable fraction (short-range ordered Si:Al-phases) showed no significant difference between HA-soils (0.48 ± 0.19 mg g⁻¹ DW) and AB-soils (0.48 ± 0.17 mg g⁻¹ DW; Figure 1d). In contrast, Al ($p < 0.001$, t-test) and Fe concentrations ($p < 0.05$, t-test) were significantly lower in HA-soils (0.86 ± 0.57 mg g⁻¹ DW for Al; 0.91 ± 0.80 mg g⁻¹ DW for Fe) compared to AB-soils (1.26 ± 0.22 mg g⁻¹ DW for Al; 2.11 ± 1.04 mg g⁻¹ DW for Fe; Figure 1d). Significantly higher Si concentrations in the bASi fraction were observed for the High Andes (3.79 ± 2.38 mg g⁻¹ DW) compared to the Amazon Basin (0.71 ± 0.48 mg g⁻¹ DW; $p < 0.001$, t-test; Figure 1e). In contrast, no significant differences were detected for Al and Fe concentrations in this fraction. Al concentrations were 0.019 ± 0.023 mg g⁻¹ DW for the High Andes and 0.02 ± 0.017 mg g⁻¹ DW for the Amazon Basin (Figure 1e). Similarly, Fe concentrations were 0.006 ± 0.004 mg g⁻¹ DW in the High Andes and 0.012 ± 0.013 mg g⁻¹ DW in the Amazon Basin (Figure 1e).

The tASi fraction revealed significantly higher Si concentrations for the High Andes (24.7 ± 14.8 mg g⁻¹ DW) compared to the Amazon Basin (9.71 ± 4.95 mg g⁻¹ DW; $p < 0.01$, t-test; Figure 1f). In contrast, Al and Fe concentrations in the tASi fraction were lower in the High Andes (0.49 ± 0.28 mg g⁻¹ DW for Al and 0.32 ± 0.29 mg g⁻¹ DW for Fe) than in the Amazon Basin (2.48 ± 3.81 mg g⁻¹ DW for Al and 0.80 ± 0.64 mg g⁻¹ DW for Fe), though these differences were not statistically significant (Figure 1f).

Notably, the cumulative mean of Al, Fe, and Si across all extracted soil fractions accounted for 4.3% of the total soil in the High Andes and 3.5% in the Amazon Basin. The largest contribution to this was Si in the tASi fraction, comprising 2.5% for the High Andes and 1% for the Amazon Basin on average.

TABLE 2 Absence/Presence of elements in minerals from soil samples detected by XRPD.

Minerals	HA-soil				AB-soil			
	Fe	Al	Si	Other	Fe	Al	Si	Other
Anatase								
Amorphous								
Chlorite								
Gibbsite								
Goethite								
Hematite								
Kaolinite								
Muscovite								
Plagioclase/Albite								
Quartz								
Rutile								
Smectite								
Talc								
Vermiculite								

4 Discussion

This study aimed to evaluate a slightly modified sequential extraction method based on (Georgiadis et al., 2015), originally developed and calibrated for temperate soils, on contrasting soils from other climatic regions that have undergone different pedogenesis. We analyzed Si, Fe, and Al in the extracts and used XRPD to detect mineral changes, assessing method validity and extractant selectivity.

XRPD data revealed marked differences in mineral composition between the soils from the High Andes (HA) and the Amazon Basin (AB). While the method provided valuable insights, we acknowledge its limitations, particularly in analyzing clay minerals and minor components due to sample constraints. The mineral composition of the HA-soils aligned with previous studies from the Urubamba Cordillera (Gabelman and Jordán, 1964; de Castro Portes et al., 2016). The HA-soil consists mainly of plagioclase/albite, amorphous phases and quartz, making up to 80% of mineral share. These minerals are partially composed of Si; the other, less abundant minerals are dominated by bonds with Si, Fe and Titan (Ti) (Table 2). For the AB-soil and other deeply weathered soils of the Amazon Region of Bolivia in Pando, and neighboring regions in Peru and Brazil, the dominance of quartz and kaolinite, as found in our XRPD analysis, is common (Osher and Buol, 1998; Marques et al., 2002; Quesada et al., 2020).

The lower limit of detection for amorphous phases by XRPD methods depends on the precision and the real accuracy of the crystalline components to be quantified by the internal standard method. The estimated standard deviation 3sigma, calculated from the correlation matrix of the parameters in the Rietveld algorithm, is in the magnitude of 2–3 mass% (Table 1). Some common sources for systematic errors like microabsorption, amorphization of crystalline

components in the milling procedure, and preferred orientation can be effectively minimized by careful sample preparation and adequate choice of the instrumental setting (Kleeberg et al., 2006). For test mixtures and preparations, the upper limit was tested to be in the range of 3–5 mass%. In the case of chemically treated soil materials it must be taken into account that changes in surface properties and dispersion may cause (i) differences in moisture adsorption resp. drying behavior, and (ii) changed disorder of layer silicates including their diffraction profiles. As the latter should be effectively included in the disorder models, the remaining systematic errors may be estimated to additional 1–2 mass%. Thus, the total uncertainties and the lower detection limit for amorphous components in soils may be given conservatively to be in the range of 5–7 mass%.

The main difference in mineral composition of the soils used were the different shares of amorphous components and the different share of quartz, which represents their difference in development stage and origin (Irion, 1978; Quesada et al., 2020). The higher share of ASi was found in the soil of the High Andes (which may be explained by volcanic ash deposition from volcanos nearby or strong ASi cycling in those natural grasslands), whereas the soil from the Amazon Basin consisted mainly of quartz. Considering Si availability, these mineral components are of major importance as ASi is a source of easily available Si and quartz represents a poorly weatherable fraction (Martín-García et al., 2015). However, the amorphous components include, besides ASi, also other X-ray amorphous soil constituents like organic matter and short-range ordered (nano-crystallin) Fe- and Al-phases. After the H₂O₂ extraction the X-ray-amorphous share of the HA-soil decreased markedly as H₂O₂ destroys OC by oxidation. This strong effect was not observed for the AB-soil which is in line with the OC contents being much lower for the AB-soil compared to the HA-soil. Thus, the decreases of the amorphous share in the HA-soil can be explained by the removal of OC, resulting in an increase of the relative share of the other components.

We found rather less plant-available Si in the soils of the High Andes in comparison to soils from the Amazon Basin, as higher temperature and precipitation foster weathering of the reactive fractions of Si. Additionally, we did not find any differences in Si bound to Fe (reducible fraction) and Al (Al-complexes) phases. We found less organically bound Si in soils from Amazon Basin due to the much lower organic matter share in those soils. Also, less bASi was found in the soil from the Amazon Basin, (amorphous share after H₂O₂ treatment) compared to the soils from High Andes. This suggests, that in High Andean soils, the relatively higher Si availability and consequently higher plant bASi production promotes a potential high cycling of bASi, resulting in greater ASi bound to the OM-fraction (H₂O₂ extractable), as phytolith are tightly bound to organic matter of plant tissue (Katz et al., 2021). More bASi may lead to higher Si dissolution, which in turn promotes the precipitation of minerogenic amorphous silica fraction (mASi), thereby increasing the tASi (Schaller et al., 2021).

For Fe contents, we found only significant differences in the Al-complexes with higher Fe contents in the soils from the Amazon Basin. Our data for the High Andes soil shows that DCB had no effect on Fe minerals (hematite) which is in line with earlier studies showing that hematite and goethite in (sub-tropical) soils are not completely dissolved by DCB treatment (Rennert, 2019). Similarly,

SROAS and Al-oxides could prevent complete reduction and extraction by DCB (Rennert, 2019).

Additionally, less plant-available Al was found in the soils from the Amazon Basin. These soils have a higher share of Al in the reducible fraction and that bound into Al-complexes (oxalate extractable). Especially the climatic conditions and the duration of weathering are determining the rate of chemical weathering of these soils: for the warm and wet tropical conditions, the availability arises from limitations in supply of fresh mineral surfaces (Edwards et al., 2017). For available and/or reactive fraction of Si, mineral weathering would be the only source on a geological time scale. In the shallower soils from the High Andes, the lower temperature and less time decreased chemical weathering, and thus release of Si.

5 Conclusion

Lately developed sequential extraction methods were established on pure minerals and have mostly been validated on soils of temperate zones. We challenged this method with soils outside of temperate climatic zones that additionally have different development stages and parent material and have been exposed to differentiated climate. For Fe and Al, convincing and logical sequential extraction protocols have already been validated across soils of the world to understand nutrient and element pools. However, XRD data shows that DCB extraction was not successful in completely dissolving hematite nor goethite for both sites.

Considering the low share of soil fractions being extracted by the different extraction methods, most of these methods (like oxalate extraction) produce data which may not be considered as solid results. The CaCl₂-method for extracting the plant available fraction is proven to be a good choice (Wu et al., 2020) as well as the Tiron method to quantify the Si concentration in the tASi fraction.

The presented results from the sequential extraction protocol for Si suggest that the CaCl₂ extraction (for plant-available Si) and a two-step protocol with density separation for biogenic Si (bASi), followed by Tiron extraction for total amorphous Si (tASi), were the most effective for the tested soils and can be recommended. Accordingly, Si sequential extraction methods appear unsuitable for reliably quantifying distinct soil silicon pools. Therefore, caution is required when incorporating data from extraction methods other than CaCl₂ or Tiron into global silicon assessments.

Data availability statement

The raw data supporting the conclusions of this article will be made available by the authors, without undue reservation.

References

- Bergmann, J., Friedel, P., and Kleeberg, R. (1998). BGMN—A new fundamental parameters based rietveld program for laboratory X-ray sources, its use in quantitative analysis and structure investigations. *CPD Newsl.* 20, 5–8.
- Cochrane, T. T., Cochrane, T. A., and Espinoza, O. E. L. (2010). Land use zoning based on a world soils and terrain digital database study to conserve the Brazil-nut forest in Bolivia's Amazonia. *Interciencia* 35, 493–499.
- Cooke, J., and Leishman, M. R. (2011). Is plant ecology more siliceous than we realise? *Trends Plant Sci.* 16, 61–68. doi:10.1016/j.tplants.2010.10.003
- de Castro Portes, R., Spinola, D. N., Reis, J. S., Ker, J. C., Costa, L. M. d., Fernandes Filho, E. I., et al. (2016). Pedogenesis across a climatic gradient in tropical high Mountains, Cordillera blanca—peruvian andes. *Catena* 147, 441–452. doi:10.1016/j.catena.2016.07.027

Author contributions

MS: Writing – review and editing, Methodology, Visualization, Writing – original draft. SK: Writing – review and editing, Investigation. RK: Methodology, Writing – review and editing. HJ: Writing – review and editing, Conceptualization. JS: Writing – review and editing, Conceptualization.

Funding

The author(s) declared that financial support was received for this work and/or its publication. The study was funded by Leibniz Center for Agricultural Landscape Research (ZALF).

Acknowledgements

The authors gratefully thank Susanne Remus for lab work and the ZALF Central lab team for analysis.

Conflict of interest

The author(s) declared that this work was conducted in the absence of any commercial or financial relationships that could be construed as a potential conflict of interest.

Generative AI statement

The author(s) declared that generative AI was not used in the creation of this manuscript.

Any alternative text (alt text) provided alongside figures in this article has been generated by Frontiers with the support of artificial intelligence and reasonable efforts have been made to ensure accuracy, including review by the authors wherever possible. If you identify any issues, please contact us.

Publisher's note

All claims expressed in this article are solely those of the authors and do not necessarily represent those of their affiliated organizations, or those of the publisher, the editors and the reviewers. Any product that may be evaluated in this article, or claim that may be made by its manufacturer, is not guaranteed or endorsed by the publisher.

- de Tombeur, F., Raven, J. A., Toussaint, A., Lambers, H., Cooke, J., Hartley, S. E., et al. (2023). Why do plants silicify? *Trends Ecol. Evol.* 3077, 1–14. doi:10.1016/j.tree.2022.11.002
- Derry, L. A., Kurtz, A. C., Ziegler, K., and Chadwick, O. A. (2005). Biological control of terrestrial silica cycling and export fluxes to watersheds. *Nature* 433, 728–731. doi:10.1038/nature03299
- Dietzel, M. (2002). “Interaction of polysilicic and monosilicic acid with mineral surfaces,” in *Water-rock interaction*. Editors I. Stober and K. Bucher (Netherlands, Dordrecht: Springer), 207–235.
- Döbelin, N., and Kleeberg, R. (2015). Profex: a graphical user interface for the rietveld refinement program BGMN. *J. Applied Crystallography* 48, 1573–1580.
- Edwards, D. P., Lim, F., James, R. H., Pearce, C. R., Scholes, J., Freckleton, R. P., et al. (2017). Climate change mitigation: potential benefits and pitfalls of enhanced rock weathering in tropical agriculture. *Biol. Letters* 13, 20160715. doi:10.1098/rsbl.2016.0715
- Espinoza Villar, J. C., Ronchail, J., Guyot, J. L., Cochonneau, G., Naziano, F., Lavado, W., et al. (2009). Spatio-temporal rainfall variability in the amazon basin countries (Brazil, Peru, Bolivia, Colombia, and Ecuador). *Int. J. Climatol. A J. R. Meteorological Soc.* 29, 1574–1594. doi:10.1002/joc.1791
- Gabelman, J. W., and Jordán, V. (1964). *Geology of the cuzco-anta-urubamaba area*. Peru: Technical Information Service.
- Georgiadis, A., Sauer, D., Herrmann, L., Breuer, J., Zarei, M., and Stahr, K. (2013). Development of a method for sequential Si extraction from soils. *Geoderma* 209, 251–261. doi:10.1016/j.geoderma.2013.06.023
- Georgiadis, A., Sauer, D., Herrmann, L., Breuer, J., Zarei, M., and Stahr, K. (2014). Testing a new method for sequential silicon extraction on soils of a temperate–humid climate. *Soil Res.* 52, 645–657. doi:10.1071/sr14016
- Georgiadis, A., Sauer, D., Breuer, J., Herrmann, L., Rennert, T., and Stahr, K. (2015). Optimising the extraction of amorphous silica by NaOH from soils of temperate-humid climate. *Soil Res.* 53, 392–400. doi:10.1071/sr14171
- Heitkamp, F., Sylvester, S. P., Kessler, M., and Jungkunst, H. F. (2014). Inaccessible Andean sites reveal human-induced weathering in grazed soils. *Prog. Phys. Geogr.* 38, 576–601. doi:10.1177/0309133314544918
- Irion, G. (1978). Soil infertility in the Amazonian rain forest. *Naturwissenschaften* 65, 515–519. doi:10.1007/bf00439791
- Katz, O., Puppe, D., Kaczorek, D., Prakash, N. B., and Schaller, J. (2021). Silicon in the soil–plant continuum: intricate feedback mechanisms within ecosystems. *Plants* 10, 652. doi:10.3390/plants10040652
- Kleeberg, R., Monecke, T., and Hillier, S. (2006). Some aspects of the preparation of samples suitable for quantitative XRD analysis. *Beiträge zur Jahrestag. Valkenberg. 4. bis 6. Oktober*, 16.
- Kleeberg, R., Monecke, T., and Hillier, S. (2008). Preferred orientation of mineral grains in sample mounts for quantitative XRD measurements: how random are powder samples? *Clay Clay Min.* 56, 404–415. doi:10.1346/ccmn.2008.0560402
- Li, Z., Meunier, J.-D., and Delvaux, B. (2022). Aggregation reduces the release of bioavailable silicon from allophane and phylolith. *Geochim. Cosmochim. Acta* 325, 87–105. doi:10.1016/j.gca.2022.03.025
- Locock, A. J., Chesterman, D., Caird, D., and Duke, M. J. M. (2012). Miniaturization of mechanical milling for powder X-ray diffraction. *Powder Diffr.* 27, 189–193. doi:10.1017/s0885715612000516
- Mamani, M., Wörner, G., and Sempere, T. (2010). Geochemical variations in igneous rocks of the Central andean orocline (13 S to 18 S): tracing crustal thickening and magma generation through time and space. *Bulletin* 122, 162–182.
- Marques, J., Teixeira, W., Schulze, D., and Curi, N. (2002). Mineralogy of soils with unusually high exchangeable Al from the Western amazon region. *Clay Miner.* 37, 651–661. doi:10.1180/0009855023740067
- Martin-García, J., Márquez, R., and Delgado, G. (2015). Relationships between quartz weathering and soil type (entisol, inceptisol and alfisol) in sierra Nevada (southeast Spain). *Eur. J. Soil Sci.* 66, 179–193.
- Mehra, O., and Jackson, M. (1958). *Iron oxide removal from soils and clays by a dithionite–citrate system buffered with sodium bicarbonate*. Clay Clay Min: Elsevier, 317–327.
- Osher, L., and Buol, S. (1998). Relationship of soil properties to parent material and landscape position in eastern Madre de Dios, Peru. *Geoderma* 83, 143–166. doi:10.1016/s0016-7061(97)00133-x
- Puppe, D., Kaczorek, D., and Schaller, J. (2022). “Biological impacts on silicon availability and cycling in agricultural plant–soil systems,” in *Silicon and nano-silicon in environmental stress management and crop quality improvement*. Elsevier, 309–324.
- Quesada, C. A., Paz, C., Oblitas Mendoza, E., Phillips, O. L., Saiz, G., and Lloyd, J. (2020). Variations in soil chemical and physical properties explain basin-wide amazon forest soil carbon concentrations. *Soil* 6, 53–88. doi:10.5194/soil-6-53-2020
- Rennert, T. (2019). Wet-chemical extractions to characterise pedogenic Al and Fe Species—a critical review. *Soil Res.* 57, 1–16. doi:10.1071/sr18299
- Schaller, J., Cramer, A., Carminati, A., and Zarebanadkouki, M. (2020). Biogenic amorphous silica as main driver for plant available water in soils. *Sci. Rep.* 10, 2424. doi:10.1038/s41598-020-59437-x
- Schaller, J., Puppe, D., Kaczorek, D., Ellerbrock, R., and Sommer, M. (2021). Silicon cycling in soils revisited. *Plants* 10, 295. doi:10.3390/plants10020295
- Schaller, J., Wu, B., Amelung, W., Hu, Z., Stein, M., Lehndorff, E., et al. (2022). Silicon as a potential limiting factor for phosphorus availability in paddy soils. *Sci. Reports* 12, 16329. doi:10.1038/s41598-022-20805-4
- Schaller, J., Webber, H., Ewert, F., Stein, M., and Puppe, D. (2024). The transformation of agriculture towards a silicon improved sustainable and resilient crop production. *Npj Sustain. Agric.* 2, 27. doi:10.1038/s44264-024-00035-z
- Schaller, J., Kleber, M., Puppe, D., Stein, M., Sommer, M., and Rillig, M. C. (2025). The importance of reactive silica for maintaining soil health. *Plant Soil* 513, 1651–1662. doi:10.1007/s11104-025-07299-5
- Souza, I. F., Archanjo, B. S., Hurtarte, L. C., Oliveros, M. E., Gouvea, C. P., Lidizio, L. R., et al. (2017). Al-/Fe-(hydr) oxides–organic carbon associations in oxisols—from ecosystems to submicron scales. *Catena* 154, 63–72. doi:10.1016/j.catena.2017.02.017
- Stein, M., Puppe, D., Kaczorek, D., Buhtz, C., and Schaller, J. (2024). Silicon extraction from x-ray amorphous soil constituents: a method comparison of alkaline extracting agents. *Front. Environ. Sci.* 12, 1389022. doi:10.3389/fenvs.2024.1389022
- Szymański, W., and Szkaradek, M. (2018). Andesite weathering and soil formation in a moderately humid climate: a case study from the Western carpathians (southern Poland). *Carpathian J. Earth Environ. Sci.* 13, 93–105. doi:10.26471/cjees/2018/013/010
- Toledo, M., Poorter, L., and Peña-Claros, M. (2011). Climate is a stronger driver of tree and forest growth rates than soil and disturbance. *J. Ecol.* 99, 254–264.
- Troll, C. (1968). “Geo-ecology of the mountainous regions of the tropical americas,” in *Geo-ecology of the mountainous regions of the tropical americas*.
- Ufer, K., Roth, G., Kleeberg, R., Stanjek, H., Dohrmann, R., and Bergmann, J. (2004). Description of X-ray powder pattern of turbostratically disordered layer structures with a rietveld compatible approach. *Z. für Kristallogr. Mater.* 219, 519–527. doi:10.1524/zkri.219.9.519.44039
- Ufer, K., Stanjek, H., Roth, G., Dohrmann, R., Kleeberg, R., and Kaufhold, S. (2008). Quantitative phase analysis of bentonites by the rietveld method. *Clay Clay Min.* 56, 272–282. doi:10.1346/ccmn.2008.0560210
- Ufer, K., Kleeberg, R., and Monecke, T. (2015). Quantification of stacking disordered Si–Al layer silicates by the rietveld method: application to exploration for high-sulphidation epithermal gold deposits. *Powder Diffr.* 30, S111–S118. doi:10.1017/s0885715615000111
- Vuong, T. X., Heitkamp, F., Jungkunst, H. F., Reimer, A., and Gerold, G. (2013). Simultaneous measurement of soil organic and inorganic carbon: evaluation of a thermal gradient analysis. *J. Soils Sediments* 13, 1133–1140. doi:10.1007/s11368-013-0715-1
- Wedepohl, K. H. (1995). The composition of the Continental crust. *Geochim. Cosmochim. Acta* 59, 1217–1232. doi:10.1016/0016-7037(95)00038-2
- Wright, A., and Bennema, J. (1965). “The soil resources of Latin America,” 1. 13–22.
- Wu, W., Limmer, M. A., and Seyffert, A. L. (2020). Quantitative assessment of plant-available silicon extraction methods in rice paddy soils under different management. *Soil Sci. Soc. Am. J.* 84, 618–626. doi:10.1002/saj2.20013